

1 **Meso-scale Simulation of Typhoon-Generated Storm Surge:**
2 **Methodology and Shanghai Case Study**

3

4 Shuyun Dong¹, Wayne J. Stephenson¹, Sarah Wakes², Zhongyuan Chen³, Jianzhong Ge³

5 ¹School of Geography, University of Otago, Dunedin, 9016, New Zealand

6 ²Department of Mathematics and Statistics, University of Otago, Dunedin, 9016, New Zealand

7 ³State Key Laboratory for Estuarine and Coastal Research, East China Normal University, Shanghai, 200062, China

8 *Correspondence to:* Wayne Stephenson (wayne.stephenson@otago.ac.nz) +64 3479 8776

9

10 **Abstract.** The increasing vulnerability of coastal mega-cities to storm surge inundation means both infrastructure and
11 populations are subject to significant threat. Planning for further urban development should include consideration of the
12 changing circumstances in coastal cities to ensure a sustainable future. A sustainable urban plan relies on sound preparedness
13 and prediction of future climate change and multiple natural hazards. In light of these needs for urban planning, this paper
14 develops a general method to simulate typhoon-generated storm surge at the meso-scale (1 - 100 km in length). Meso-scale
15 simulation provides a general approach with reasonable accuracy that could be implemented for planning purposes, while
16 having a relatively low computation resource requirement. The case study of Shanghai is used to implement this method. The
17 meso-scale simulations of two historical typhoon not only provides realistic typhoon storm-surge inundation results at the city
18 level but is also suitable for implementing a large number of simulations for future scenario studies. The method will be
19 generally applicable to all coastal cities around the world to examine the effect of future climate change on typhoon-generated
20 storm surge, even when historical observation data is inadequate or not available.

21 **Keywords** Storm surge, typhoon, meso-scale, simulation; Shanghai

22 **1 Introduction**

23 Rapid urban expansion in coastal mega-cities (cities with populations over 10 million) leads to increased land demand and
24 vulnerability to hazards for significant numbers of people who are economically and socially disadvantaged. It is necessary to
25 be well prepared and plan to ensure a sustainable future for these cities (Timmerman and White 1997; Jiang et al. 2001; Yeung
26 2001). Typhoon-generated storm surge is a major hazard for many coastal cities and leads to significant economic losses.
27 Considering the ongoing coastal development and population growth in coastal mega-cities, preparedness and urban planning
28 play a critical role in coastal management and hazard mitigation. Therefore, the increasing vulnerability of coastal mega-cities
29 to storm surge inundation needs be assessed to improve the resilience of these cities (Woodruff et al. 2013; Aerts et al. 2014;).
30 Many integration models for typhoon and storm surge have been developed and applied to simulate regional storm surge
31 inundation and analyse its impact (Flather et al. 1998; Lowe et al. 2001; Choi et al. 2003; Jakobsen and Madsen 2004;
32 Westerink et al. 2008; Zhang et al. 2008; Davis et al. 2010; Elsaesser et al. 2010; Dietrich et al. 2011a,b; Zheng et al. 2013).
33 In order to achieve more accurate results, high resolution mesh and data are usually employed in these models requiring a large
34 amount of computing time and consequently the application of such models are limited to small regions. As suggested by Aerts
35 et al. (2014), existing hydrological models for inundation scenarios usually need to be adjusted for application at the regional
36 level. A high-resolution storm surge model could therefore be too time consuming to be used for planning purposes when a
37 large number of simulations need to be undertaken to gain a better knowledge of storm surge inundation. Ogie et al. (2019)
38 argued that there is a need for less data rich approaches to flood modelling of coastal mega-cities where there is often a paucity
39 of data. The purpose of this paper is to develop a less resource intense simulation method for typhoon storm surge inundation
40 at a city scale and to implement this method using Shanghai as a case study. The approach developed was to conduct numerical
41 simulations of typhoon and their associated storm surge at a meso-scale (1 - 100 km in length), which can then be utilized to
42 compute flooding scenarios.

43
44 Previous storm surge modelling can be divided into three types based on scale of modelling, namely large-, meso-, and small-
45 scale. For large scale studies, these usually concentrate on simulating storm surge at the national level (>100 km in length).
46 For example, Lowe et al. (2001) developed a storm surge with 35 km resolution for the North west European continental shelf
47 region, and then analysed the effects of climate change using a regional climate model. Due to the high risk of storm surge,
48 there have been studies conducted for the Louisiana coast, USA (Westerink et al. 2008; Wamsley et al. 2009; Sheng et al.
49 2010; Butler et al. 2012;) and the Gulf of Mexico area (Dietrich et al. 2011a,b; Dietrich et al. 2012;). These large-scale storm
50 surge studies normally apply a large spatial resolution, 50 – 100 km on average, to allow the simulation to be run smoothly in

51 a large-scale area. It is inevitable that at such large spatial resolution variations in storm surge level at the regional scale is lost,
52 making it a less suitable model for studying the impact of inundation at a city scale (typically 20-80 km length of coast). Meso-
53 scale storm surge modelling typically focuses on a scale of 1 - 100 km in length. Shepard et al. (2012) demonstrated a method
54 to assessing community vulnerability of the southern shores of Long Island, New York to storm surge. For small-scale storm
55 surge studies, the focus is at a regional level (1 – 1000 m in length). Funakoshi et al. (2008) developed a fine small-scale storm
56 surge model for the St. Johns River Basin in USA. Xie et al. (2008) developed storm surge modelling to simulate the
57 corresponding inundation. Frazier et al. (2010) examined the socioeconomic vulnerability to storm surge in Sarasota County,
58 Florida, USA. Small-scale storm surge studies normally focus on the effect of storm surge at a local level and is commonly
59 used to provide advice for small-scale planning and emergency management.

60 There are a number of storm surge studies conducted in China, and hydrological models for storm surge simulation have been
61 developed. However, these are either at a large or small-scale, which may lead to a loss of spatial resolution in the simulated
62 storm surge results or in huge costs in computation time. Most of these studies emphasized the significance of numerical
63 modelling of storm surge and risk analysis either for the coastline on a large spatial scale or for the local coastal area with fine
64 resolution simulation. For example, Zheng (2010) developed a numerical model to simulate storm surge under the effects of
65 tide and wind wave for the coast of China. In 2011, Tan et al. (2011) assessed the vulnerability of coast cities in China to storm
66 surge using an indicator system. Yin (2011) also assessed the risk to typhoon storm surge based on the simulated results from
67 large scale storm surge model and a proposed indicator system for the coast of China. Other studies placed emphasis on the
68 analyse of storm surge at small regional scale areas along the Chinese coast (e.g. Zhang et al. 2006; Xie 2010; Xie et al. 2010;
69 Ye 2011).

70

71 This study therefore, utilizes a meso-scale (between large and regional scales) approach for inundation vulnerability to typhoon
72 storm surge to improve knowledge of inundation vulnerability and to guide future vulnerability mitigation strategies.
73 Moreover, a large amount of simulations are involved in planning. Therefore, in order to fit this purpose, a meso-scale study
74 for Shanghai is utilized, filling the gap between the small and large-scales of previous studies. In addition, this meso-scale
75 simulation aims to demonstrate a general approach that could be easily implemented for other coastal cities, and has much
76 lower requirements for computation time and data than previous approaches.

77 **3 Data and Methods**

78 The objective of this general methodology for simulating typhoon storm surge inundation is to develop an adaptable procedure
79 that allows numerical simulations to be carried out easily in coastal cities around the world. Firstly, the data required in the
80 typhoon and storm surge simulations was assembled, including the observation data from typhoon, tidal constituents,
81 topography, and land use data. Two historical typhoon were selected to develop typhoon profiles and then wind and pressure
82 fields were calculated to drive the hydrodynamic storm surge model. Typhoon wind and pressure field was calculated based
83 on historical typhoon profiles. Moreover, tidal observed data was collected to validate the hydrodynamic models in the next
84 step. The next step was to implement a storm surge model to simulate the generation and propagation of typhoon-driven storm
85 surge model at coastal and regional scales. The historical wind and pressure fields are inputs into the coastal hydrodynamic
86 model along with the tidal constituents as key driving factors to simulate the initial current and wind-induced surge at coastal
87 scale. Then, considering river discharge and coastal protection works, storm surge is simulated using the regional
88 hydrodynamic model with a fine spatial resolution unstructured mesh. Lastly, the flood depth can be extracted from the

89 simulation results in regional hydrodynamic model and overlaid onto the urban digital elevation model, where the flood depth
90 and its spatial extent are displayed on a two-dimension flood map. The proposed method is explained in following sections.

91 **3.1 Assembling Data**

92 An accurate wind and pressure field has been identified as having an important role in storm surge modelling (Bode and Hardy
93 1997). In order to provide wind and pressure field to drive storm surge in hydrodynamic model, historical typhoon data needs
94 to be collected from records. There are various types of typhoon data, such as best track data, observed data, and satellite data.
95 Typhoon wind and pressure field are calculated in this framework by applying the parametric model built in MIKE 21 Cyclone
96 Wind Generation tool. Typhoon data required in the simulation then are the typhoon track, the central and neutral air pressure,
97 and the maximum wind speed. This data can usually be found in best track data published by meteorological agencies (Ying
98 et al. 2014) or satellite reanalysis database (Simmons et al. 2007). The development and optimization process of typhoon wind
99 modelling is described in Section 3.3. To pre-process the data for the subsequent modelling, all the historical topography and
100 meteorological data was digitized into appropriate formats, including bathymetry, urban digital elevation model, land use map,
101 and coastal engineering features. In this step, tide constituents are prepared in the format that is required in storm surge
102 modelling.

103 **3.2 Developing a Storm Surge Coupled Model**

104 Water propagation at the coast is significantly sensitive to surface wind forcing and astronomic tides, especially during typhoon
105 events. As suggested by Huang et al. (2010), wave-induced forces on storm surge are incremental, so there is no need to utilise
106 an independent wave model. Therefore, in this study, a coupled model will be built to simulate storm surge. In order to provide
107 accurate wind and pressure fields and tide influence for the coastal and regional circulation, a two-domain, Typhoon Storm
108 Surge Model was set up, covering the coastal and regional geographic scales. In this method, MIKE 21 was chosen to simulate
109 typhoon-generated storm surge with consideration of river discharge and coastal protection works. As commercial software,
110 MIKE 21 has broad applicability and a low requirement of specialized knowledge. In general, a hydrodynamic model for a
111 coastal area will be set up and calibrated against observed tide data. Then the coastal hydrodynamic storm surge model will be
112 utilized to calculate the corresponding distribution of the wave field under the influence of a historical typhoon wind and
113 pressure field. On this basis, a regional storm surge model can be built for shallow water to consider wave refraction,
114 diffraction, and transformation in order to calculate storm surge in the area of interest. After calibration against measured
115 historical data of storm surge, this model can be applied to project the impact of future storm surge for the study area.

116 **3.2.1 Grid Model and Resolution**

117 In order to precisely simulate storm surge in any coastal area, a fine grid model with appropriate resolution should be
118 constructed for the coastal terrain and topography. The grid greatly affects the generation, propagation and reflection of the
119 wave, and bottom friction. However, a very fine grid resolution causes significant increases in the computing time and resource.
120 Thus, a balance between accuracy of numerical simulation and the computing requirement should be achieved in the model.
121 The resolution of the unstructured mesh applied in the coastal hydrodynamic model is recommended to be set in a range of 1
122 km at the coastal zone to 10 km at the open ocean boundary (Fig 1). For the regional hydrodynamic model, the resolution can
123 be more precise with an average of 300 m.

124 **3.2.2 Coastal Hydrodynamic Model**

125 Typhoon wind and pressure fields, astronomical tide and waves are the main factors of storm surge that need to be simulated
126 (Savioli et al. 2003). Combining the statistical hydrological and meteorological data, a coastal typhoon storm surge model is

127 designed and developed using MIKE software to simulate historical storm surge events, which in turn allows simulation of the
128 hydraulics, waves and related phenomena in the coastal area. This coastal hydrodynamic model with a flexible mesh is built
129 up in the MIKE 21 flow model to simulate wind-generated waves and current conditions with respect to pre-processed tide,
130 wind and pressures fields. This coastal typhoon storm surge model was first calibrated under normal circumstances to fit no
131 storm tidal conditions, then run for historical typhoon storm surge events to ensure reliability. First, the coupled model was
132 only run to compute tide parameters during the three days before the typhoon for the entire region for the purpose of calibration.
133 Then the model was run to simulate historical typhoon events and the simulation calibrated with observed data of surge
134 elevation. In addition, computed data of wind speed and direction were calibrated against satellite data or local measured data.

135 3.2.3 Regional Hydrodynamic Model

136 Based on the computed data from the coastal hydrodynamic model, a regional model was developed to simulate the movement
137 of typhoon-induced surge for a relatively small regional area. Then this regional model was run for different scenarios, to
138 project the effects of global climate change and land subsidence on the regional storm surge level. This regional hydrodynamic
139 model can provide predicted results under various scenarios for decision making, hazard mitigation and emergency evacuation
140 planning. By analysing various future scenarios, a better understanding of coastal vulnerability can be reached, then appropriate
141 preparedness and mitigation planning can be made.

142 3.2.4 Major Model Parameters

143 The hydrodynamic module in MIKE 21 Flow Model was employed in this study to implement the coastal and regional
144 hydrodynamic models. A number of model parameters need to be set ahead of running simulations, so these are now described.
145 The horizontal eddy viscosity is specified as a constant of 0.8 is taken from Smagorinsky, (1963) and used in the SC-TSSM
146 (Shanghai Coastal Typhoon Storm Surge Model). The effect of different shapes of sea walls in the storm surge model is minor,
147 therefore the shape of the sea wall was assumed to be trapezoidal. In our case study below, the height of the sea wall along the
148 Shanghai coastline is 6.37 m relative to mean sea level and this value is used in the model. Boundary conditions in the open
149 sea are driven by the astronomical tide. In this study, the tide profile before and during typhoon period was computed by the
150 Global Tide Model in MIKE. TOPEX/POSEIDON altimetry data have been employed in the Global Tide Model with a spatial
151 resolution of $0.25^\circ * 0.25^\circ$. The output data of boundary condition files have a 1-hour interval. Other parameters configured
152 in the coastal and regional hydrodynamic models are listed in Table 1.

153 3.3 Storm Surge Inundation Modelling

154 For large-scale and meso-scale studies, storm surge inundation mapping can be conducted to predict the inundation depth and
155 spatial extent. The approach to inundation mapping can also be utilized for the purpose of further planning which aims to
156 predict the distribution of storm surge inundation, especially in land reclamation planning. Based on the typhoon storm surge
157 simulation results from the regional hydrodynamic model, inundation maps are constructed using ArcGIS. Flood maps drawn
158 in ArcGIS provide graphic information with which to analyse the differences in inundation depth across the city.

159 3.4 Optimizing Process in Wind Field Simulation by MIKE Software

160 In order to analyse the storm surge caused by typhoon, a precise simulation is closely bound to the accuracy of wind and
161 pressure field specification. It is therefore of considerable significance that a specific, accurate and representative typhoon
162 field is input into the typhoon model. In this study, the wind and pressure field of the typhoon was generated by the parametric
163 model in the MIKE 21 Cyclone Wind Generation tool. There are four parametric models built in this tool; Young and Sobey
164 (Young and Sobey 1981), Holland (Holland 1980), Holland for double vortex (Harper and Holland 1999), and Rankine (1872).

165 The Holland model has been chosen to simulate the typhoon wind field in the Shanghai case study because the adjustability of
166 the Holland parameter B allows the model to be modified to fit existing data more realistically.

167 Most of the parameters in the Holland model can be collected from the typhoon best track dataset of the China Meteorological
168 Administration and the European Centre for Medium-Range Weather Forecasts (ECMWF) (Molteni et al. 1996). The best
169 track data were recorded every 6 hours, then the model will simulate the wind and pressure field at 1-hour interval. The
170 remaining two parameters, the radius of maximum wind R_{mw} and parameter B , was calculated by Eq. (1) (Ge et al. 2013) and
171 Eq. (2) (Vickery et al. 2000) respectively.

$$172 \quad R_{mw} = (7.5757576 \times 10^{-5}) \times P_c^2 - 0.50560606 \times P_c + 477.01515 \quad \text{Eq. (1)}$$

$$173 \quad B = 1.38 - 0.00184|P_c - P_n| + 0.00309R_{mw} \quad \text{Eq. (2)}$$

174 where P_c represents the pressure at the typhoon centre or central pressure, P_n is the ambient pressure field or neutral pressure.

175 Although the computed results by the Holland model show that the model is in good agreement with the actual observation, a
176 relative error remains in the computation after typhoon landfall (Fig. 1). Compared to the observation data, the computed wind
177 speeds fall rapidly after the typhoon made landfall. In order to improve the quality of typhoon simulated results, a commonly
178 applied approach is to blend computed wind speeds results with satellite reanalysis database, such as global National Centres
179 for Environmental Prediction and National Centre for Atmospheric Research (NCEP/NCAR) Reanalysis data and ECMWF
180 reanalysis dataset (Dutta et al. 2003; Jia et al. 2011). The ECMWF reanalysis dataset has a better spatial resolution of 0.25°
181 than NCEP/NCAR (2.5°). Therefore, the ECMWF dataset was chosen here as the background wind field to achieve a more
182 precise result at the outer area of the radius of maximum wind.

183

184

185

186

187

188

189

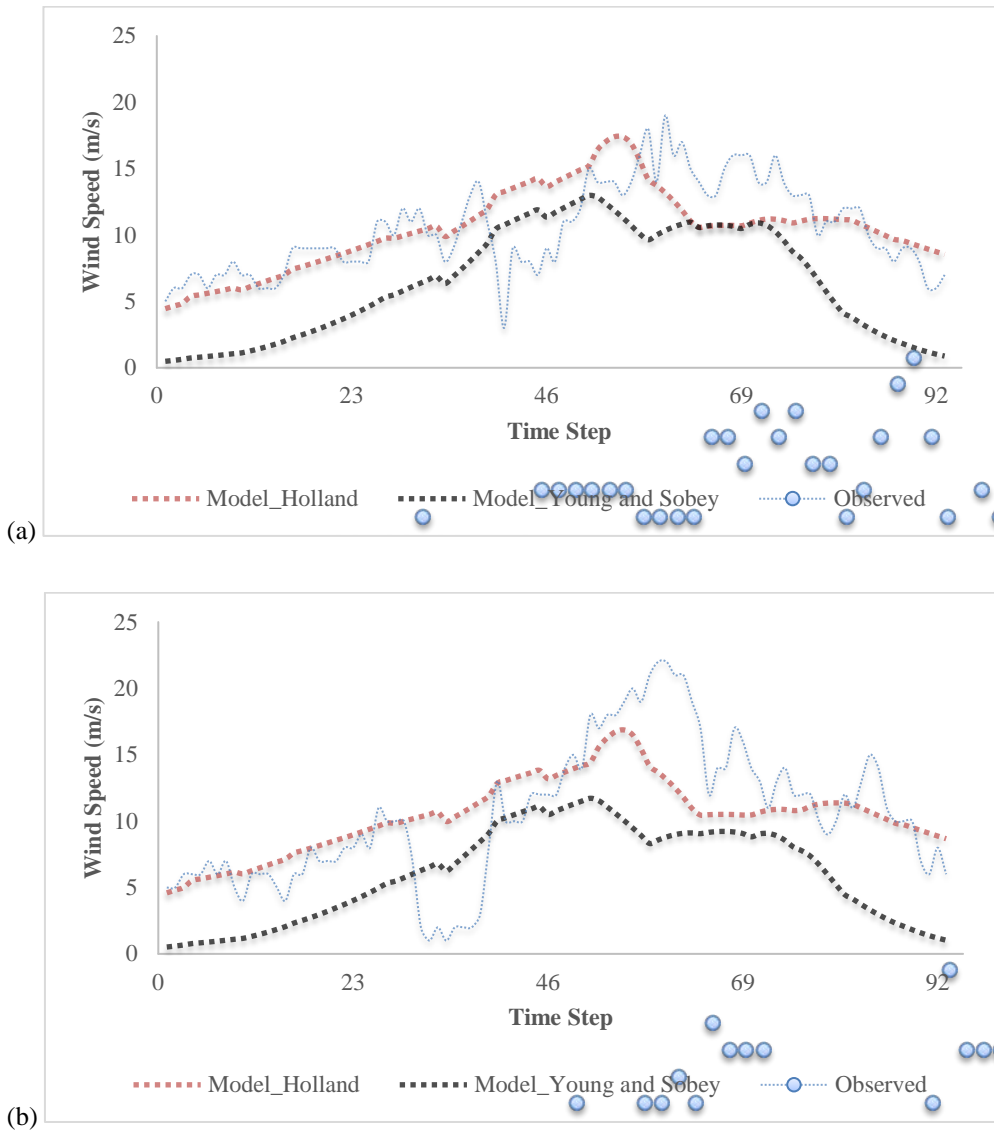


Fig. 1 Model data comparison for (a) results at Tanxu station, and (b) results at Daji station. The blue points indicate the observation data, the red curve shows the simulated results following the Holland model, and the grey curve represents the results computed by the Young and Sobey model.

190 The ECMWF reanalysis dataset is a continually updating dataset with the finest resolution of a $0.25^\circ * 0.25^\circ$ grid mesh
 191 presented by the European Centre for Medium-Range Weather Forecasts. It has been recording joint data from diverse,
 192 advanced, operational, numerical models, representing the state of the Earth's atmosphere, incorporating observations and a
 193 numerical weather prediction model four times daily since 1948 (Simmons et al. 2007). As a result of the assimilation of the
 194 observational data, the recorded atmospheric circumstances in the ECMWF dataset can be regarded as providing a close
 195 approximation of the state of the atmosphere (Molteni et al. 1996). Therefore, the ECMWF can provide a precise, nearly real
 196 atmospheric background for adjusting the Holland model.

197 In order to integrate the strong points of the MIKE software and the ECMWF reanalysis dataset, the MIKE Software
 198 Development Kit (SDK) is used here to optimize the simulation results from the MIKE 21 Cyclone Wind Generation Tool.
 199 The wind speed $V(r)$ at a distance r from the centre of the typhoon, can be given by Eq. (3):

200

201

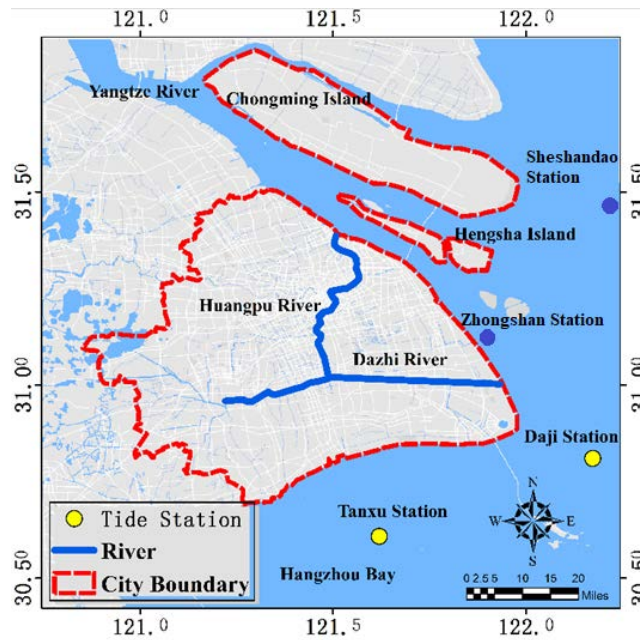
202

$$V(r) = \begin{cases} V_{MIKE} & , r < R_{mw} \\ V_{ECMWF} & , r > R_{mw}, \\ \alpha V_{MIKE} + (1 - \alpha)V_{ECMWF}, & r = R_{mw} \end{cases} \quad \text{Eq. (3)}$$

204 where V_{MIKE} is the wind speed calculated by the MIKE 21 Cyclone Wind Generation Tool, V_{ECMWF} is the wind speed
 205 computed from the ECMWF interpolation results, and α is the weight factor in order to smooth rough edges. An optimized
 206 coupled wind and pressure field can be generated by programming in the MIKE SDK based on Eq. (3). This produced a wind
 207 and pressure field that matched the actual typhoon event well.

208 4 Case Studies in Shanghai

209 Following the proposed framework for assessing inundation vulnerability to storm surge, a case study of Shanghai is used to
 210 examine the application of this proposed approach (Fig. 2). There were 16 major storm surge events in Shanghai from 1905 to
 211 2000; five of them (in 1905, 1933, 1981, 1997, and 2000) have led to severe flooding and billions of Yuan in economic damage.



212

213 **Fig. 2** Local map of Shanghai with the red dash line indicating city political boundary and simulation area, while the blue line
 214 indicating the Huangpu and Dazhi Rivers. The yellow points represent two tide gauges used to calibrate the models, while the
 215 blue points represent tide gauges used for tide validation. Sources: Esri, DeLorme, HERE, USGS, Intermap, iPC, NRCAN,
 216 Esri Japan, METI, Esri China (Hong Kong), Esri (Thailand), MapmyIndia, Tomtom

217

218 Along the Shanghai coast, land reclamation has grown substantially due to the increasing demand for land for further urban
 219 development, about 480 km² land was been claimed in Shanghai between 1954 and 1990 (Shanghai Nongken Chronicles
 220 Compilation Committee 2004). Reclaimed land can alleviate the pressure on land that results from the continuous growth of
 221 cities in the process of rapid expansion. Most of the newly reclaimed land has been used for agriculture and industry (Shanghai
 222 Municipal Planning and Land & Resources Administration 2010). However, such extensive reclamation activities requires
 223 long-term, well-developed planning, otherwise there may be increased vulnerability and even catastrophic damage due to
 224 natural hazards.

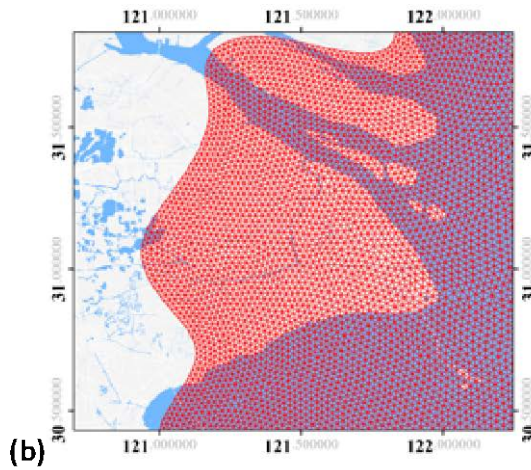
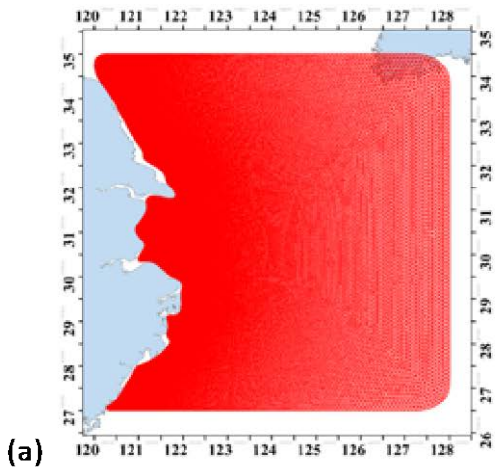
225 Typhoon Winnie in August 1997 and Typhoon Wipha in September 2007, were chosen as case studies to simulate typhoon
226 storm surge and assess the vulnerability to typhoon storm surge inundation.. Both Winnie and Wipha were categorised as super
227 typhoon by the China Meteorological Administration and caused serious storm surges in Shanghai. These two typhoon affected
228 a wide-ranging area, so simulation results could provide more information on the vulnerability of different land use types under
229 worse case scenarios. In addition, Winnie and Wipha represented typical turning track typhoon. They developed in the northern
230 Pacific Ocean, and then moved north-west towards China. After they across the East China Sea, they moved north-eastward.
231 As with the majority of typhoon affecting Shanghai, although they did not make landfall directly at Shanghai, they generated
232 high storm surge in Shanghai, 5.72 m during Winnie and 3.39 m during Wipha. In addition, the 10 years between these two
233 typhoon could allow the simulations to reveal how inundation vulnerability of different land use types to typhoon storm surge
234 changed over time.

235 Typhoon Winnie (1997) was an especially large and devastating typhoon. After passing north of Taiwan, Winnie made landfall
236 at the south-east of Shanghai in Wenling, Zhejiang province on 18 August 1997. Its centre was never closer than 400 km from
237 Shanghai, however the storm surge caused by Winnie led to extraordinary levels of flooding. Winnie caused 212 deaths, over
238 1 million people were displaced, and there was 4.1 billion yuan of economic losses (State Oceanic Administration 1989-2015).
239 A resulting storm surge of up to 6.57 m was measured at Jinshanzui Station. After landfall, Winnie shifted from the northeast
240 to northwest, giving rise to approximately 37 km of riverbank overflowing and 70 km of dike breaches (Zhu et al. 2002). A
241 storm surge of approximately 7.9 m developed in Zhejiang province, then this decreased to around 5.72 m as it approached
242 the Shanghai area. Typhoon Wipha (2007) was another destructive typhoon which passed near Shanghai and landed in
243 Cangnan, Zhejiang province on 19 September 2007. As a turning track typhoon, it passed to the west of Shanghai after making
244 landfall to the south . Although the eye of the Wipha did not pass near Shanghai, its outer strong wind and rain bands resulted
245 in severe flooding to Shanghai. Although the recorded highest water level in Shanghai was only 3.39 m during this typhoon
246 on 19 September 2007, 128 roads flooded and over 1 million Yuan (2007) of direct losses were caused in Shanghai. Almost
247 300,000 people had to be evacuated by the Shanghai government (State Oceanic Administration 1989-2015).

248 **4.1 Required Data and Processing**

249 Topography and meteorological data for Shanghai in both 1997 and 2007 were collected and processed before modelling.
250 Best track assimilated wind data was obtained from the China Meteorological Administration Tropical Cyclone Data Centre
251 and ECMWF Global Reanalysis Products with a resolution of 0.25 °. Both datasets have a 6-hour interval, therefore integrate
252 well with each other in the typhoon model helping to improve the accuracy of simulated results.

253 The computational models in this study employ an unstructured mesh spacing of 1 km in the regional area and 100 km for the
254 open sea area. The topographical data applied in the urban area to generate the flexible mesh was provided by the East China
255 Normal University. The topographical data was extracted from the digital elevation model of Shanghai with a 5 m spatial
256 resolution. Bathymetry was taken from the ETOPO1 Global Relief Model downloaded from NOAA with a grid resolution of
257 1 arc-minute in the open sea area, while data provided by the East China Normal University with a spatial resolution of 1 km
258 were adopted to improve the accuracy of the bathymetry data near shore (Fig. 3).



(a)

(b)

259

260 **Fig. 3** Shanghai Coastal Storm Surge Model with the resolution varying from 10 – 100 km. (a) shows the unstructured mesh
 261 with the differing resolution, ranging from 10 – 100 km. (b) provides an enlarged image of the mesh around Shanghai. Sources:
 262 Esri, DeLorme, HERE, USGS, Intermap, iPC, NRCAN, Esri Japan, METI, Esri China (Hong Kong), Esri (Thailand),
 263 MapmyIndia, Tomtom

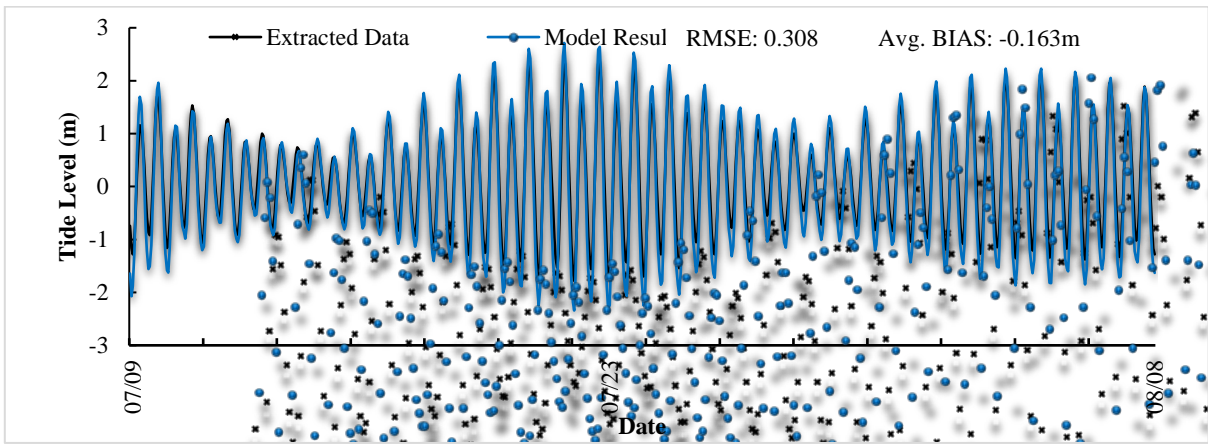
264

265 Four tide gauge stations were utilized here to validate and calibrate the simulated results from the typhoon and storm surge
 266 models. For the purpose of model validation, the SC-TSSM was run for a period of one month before both historical typhoon
 267 events. In these simulations, the effect of wind forcing was not taken into account in order to compare the plain model results
 268 with actual data at the Sheshandao and Zhongjun Stations, since observed tide levels at these gauge stations are not available
 269 during the selected typhoon events. In order to validate the coastal storm surge model, the tide level extracted from a tide table
 270 was adopted. The comparison between extracted data and simulated data is shown in Figure 4. From Figure 4, the SC-TSSM
 271 simulations show good agreement with the extracted data from the two gauge stations. At Sheshandao and Zhongjun Stations,
 272 overall errors of 3.30 % and 0.52 % occurring during Winnie and Wipha respectively. Computed wind and storm surge results
 273 from numerical models have been calibrated based on observation data at the two gauge stations off the coast of Shanghai, at
 274 Daji and Tanxu Stations (Fig. 2).

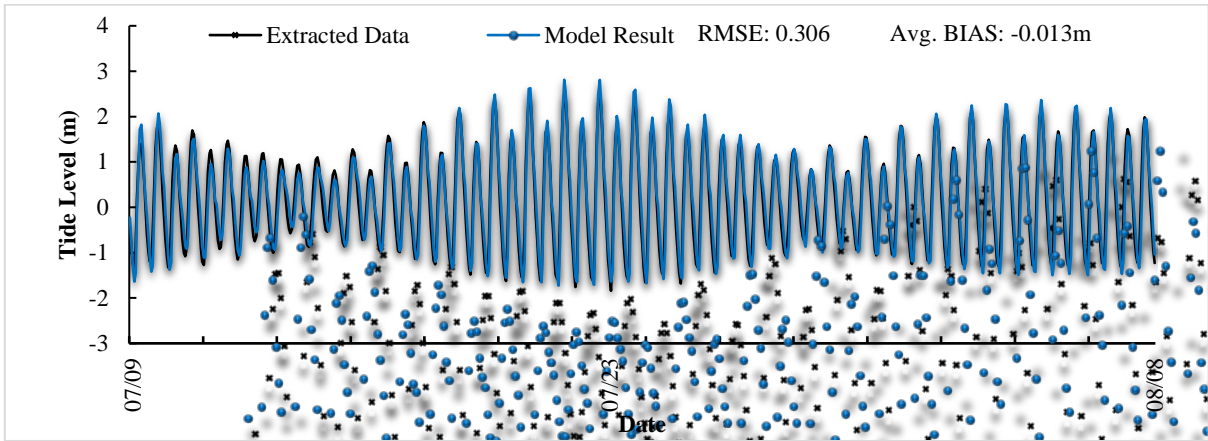
275

276

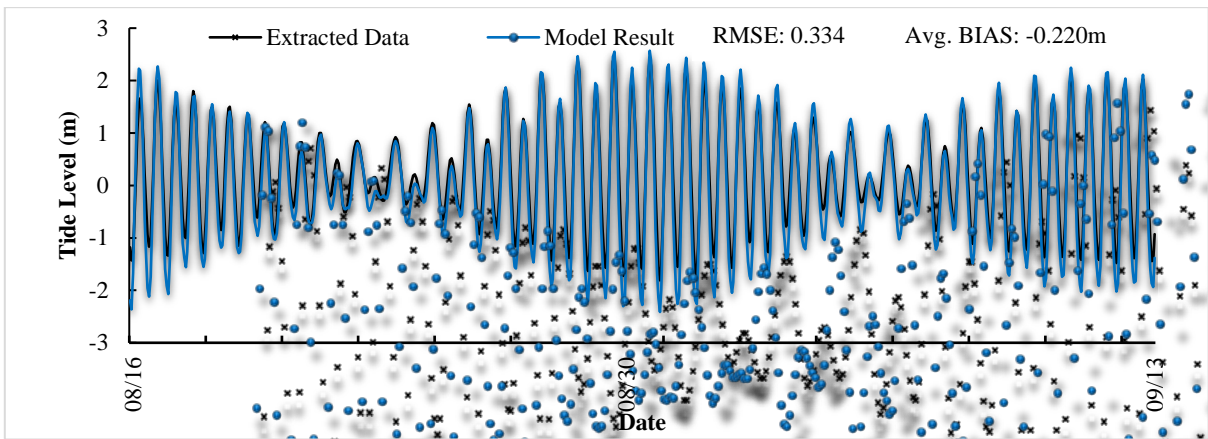
277



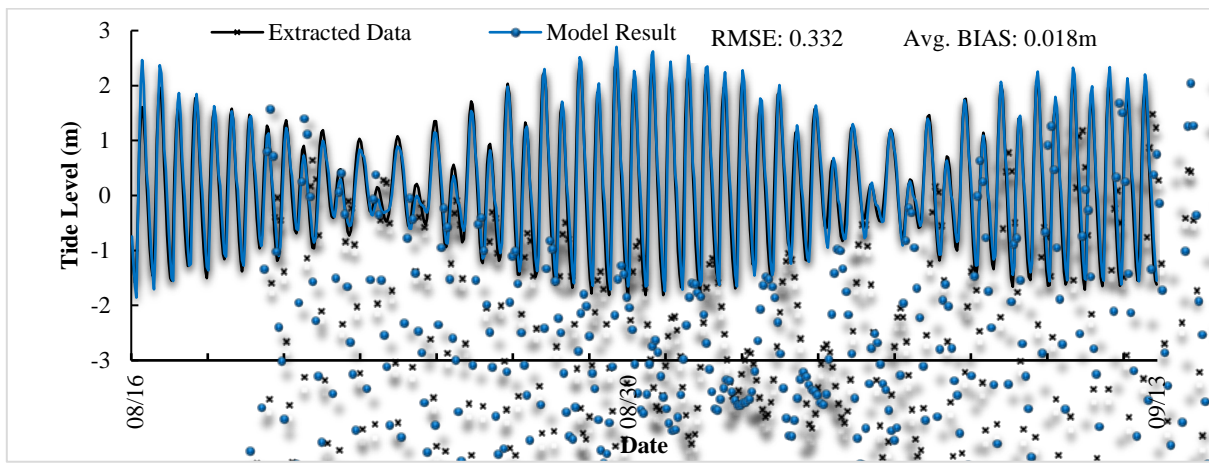
(a) one month before Typhoon Winnie at Sheshandao Station



(b) one month before Typhoon Winnie at Zhongjun Station



(c) one month before Typhoon Wipha at Sheshandao Station



(d) one month before Typhoon Wipha at Zhongjun Station

278 **Figure 4** Time series of tide level (unit: m) at the tide gauge stations (Sheshandao and Zhongjun Station) presented in Figure
 279 2. (a) and (b) present tide level at Sheshandao and Zhongjun Station from 8 July 1997 to 8 August 1997 before Typhoon
 280 Winnie, while (c) and (d) present tide level at Sheshandao and Zhongjun Station from 15 August 2007 to 15 September 2007
 281 before Typhoon Wipha. The black line indicates the extracted data, while the computed results from the SC-TSSM are shown
 282 with the blue line.

283

284 4.2 Typhoon Modelling

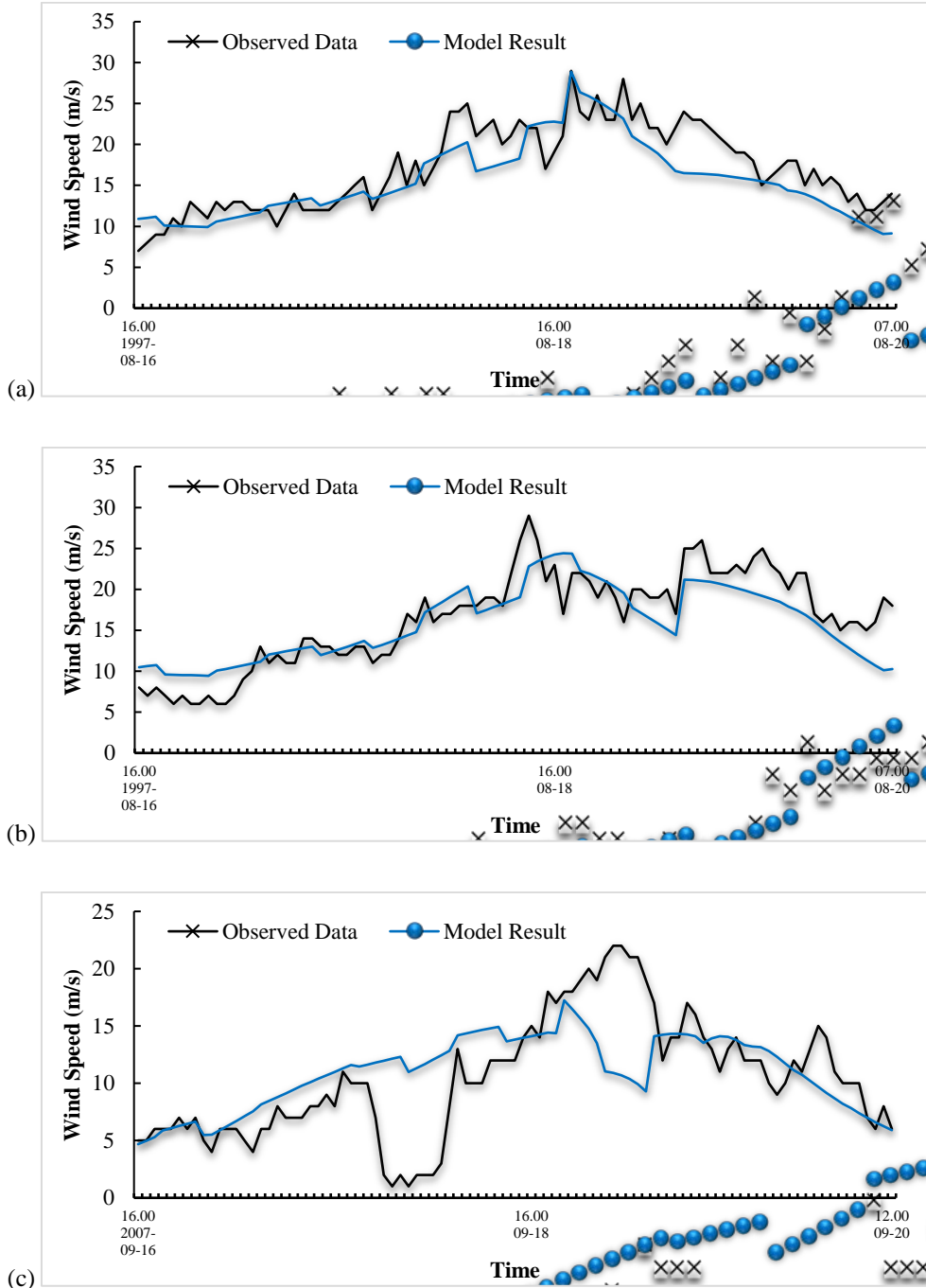
285 In this study, the impacts of typhoon are derived from the wind and pressure fields using the MIKE 21 Cyclone Wind
 286 Generation tool. In order to improve the accuracy of the simulated results, the reanalysis dataset from ECMWF has been
 287 applied in MIKE SDK. Details are given in the following sections regarding the setup, calibration, and computed results of
 288 Typhoon Winnie and Wipha.

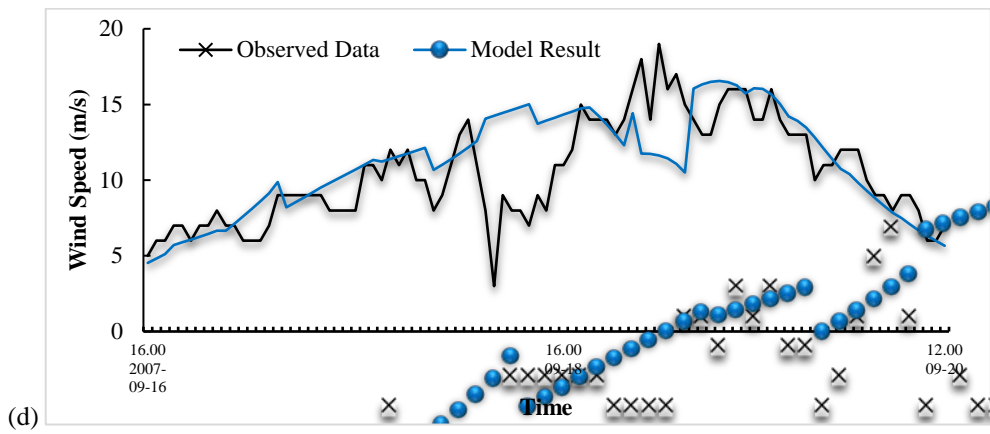
289 The typhoon model produces an output with a 1-hour interval, including the air pressure, and U and V components of wind
 290 speed. Afterwards, the simulated results have been passed to the storm surge model to generate wind-induced waves. The
 291 dataset used to initialize and, subsequently, simulate wind and pressure field in MIKE 21 was extracted from the best track
 292 data published by the CMA Tropical Cyclone Data Centre. The data for model optimization in MIKE SDK were a ECMWF
 293 reanalysis dataset with 6-hour intervals and a resolution of $0.25^\circ \times 0.25^\circ$. In this study, the wind and pressure fields were
 294 generated with the parametric model of Holland's wind field profile for the area between $30 - 35^\circ$ N, $120 - 130^\circ$ E. ETOPO1
 295 data and local measured data were employed to develop a topographical profile of the entire coastal domain.

296 The Holland parameter B was set using Eq 2. . A geostrophic correcting parameter can be implemented as a constant or varied
 297 according to the wind speed at different places. In order to correct the asymmetrical forward movement of a tropical cyclone,
 298 a correction factor δ_{fm} and the maximum angle of cyclone movement are introduced into the model to adjust the wind profile.
 299 In the case of Shanghai, δ_{fm} was set to 1 as recommended in the MIKE 21 user manual. The maximum angle was set to 115°
 300 and 150° as the maximum angles of Winnie's and Wipha's movements, respectively. Observed data from two meteorological
 301 stations (Daji and Tanxu) have been used to calibrate the typhoon model. Results were outputted from the Holland model at 1
 302 hr intervals and compared against observed data (Figs. 5 and 6). For both typhoon, calibration results of wind speed show that
 303 the simulation agrees well with measured data before each typhoon made landfall at Daji and Tanxu. After the landfall, the

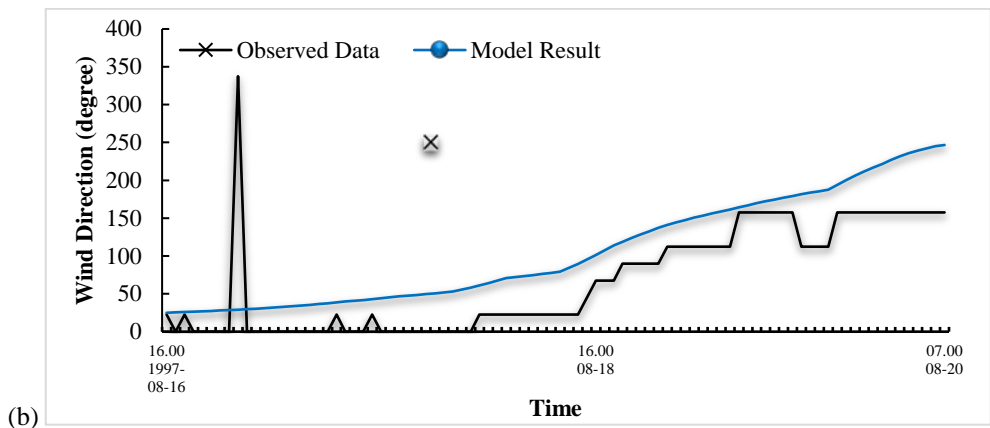
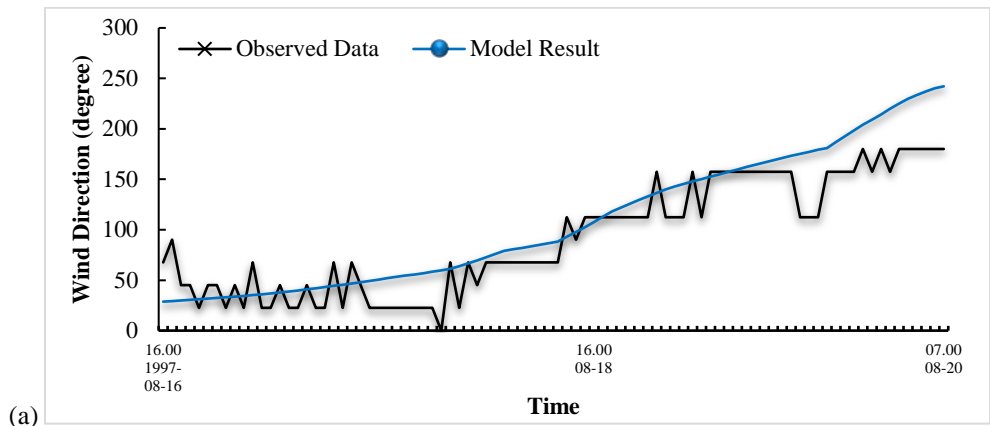
304 simulation shows a 17.9 % and a 14.4 % mean absolute percentage error against observed data. The reason for this large
305 increase in the error after landfall is mainly the long distance between the track of both typhoon and the meteorological stations.
306 In addition, previous studies suggested significant fluctuations during typhoon events may be related to regional wind fields
307 rather than the wind field driven by the typhoon (Zhu et al. 2002). Thus, the simulations around these two meteorological
308 stations failed to capture such fluctuations in wind speed. Although the simulated data cannot reflect minor changes in wind
309 direction at shorter time intervals, they still have the same trend as do the observed data (Fig. 5). After calibration of the model,
310 the computed results have been passed to MIKE SDK, and integrated with ECMW.

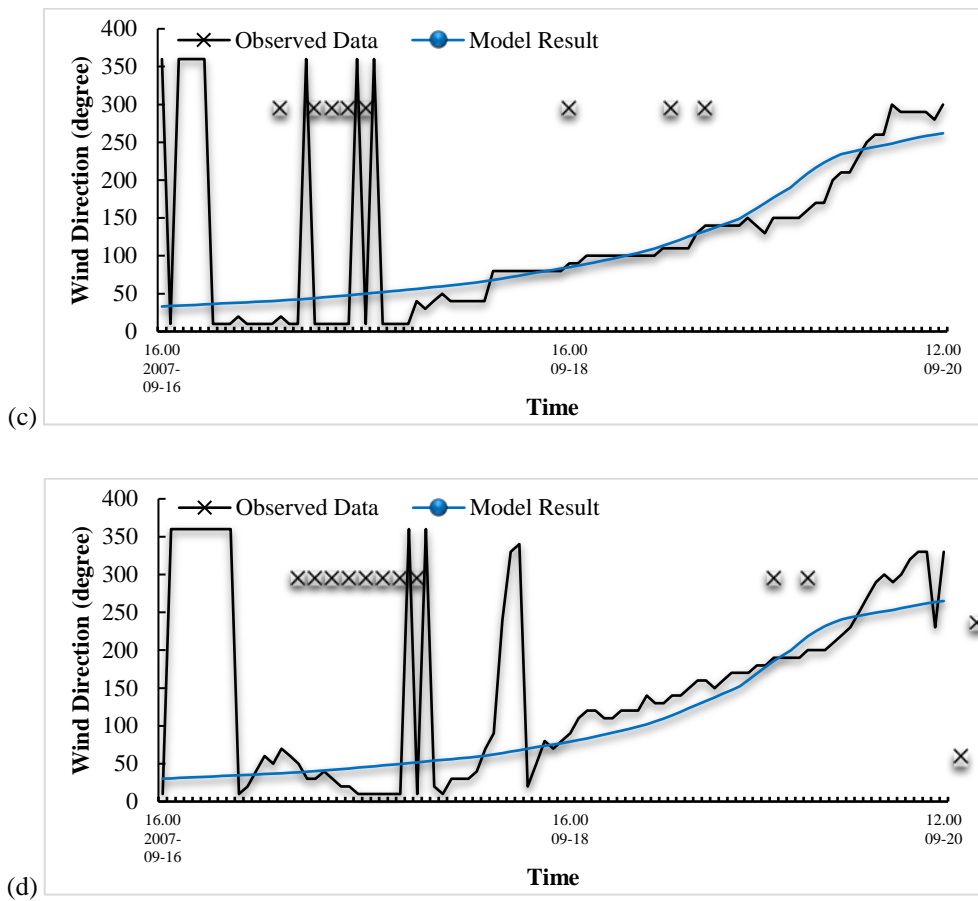
311





312 **Fig. 5** Data comparison between computed wind speed (m/s) and observed data at the two wind gauge stations in Shanghai
 313 during Typhoon Winnie and Wipha. The blue line presents the simulated results from the typhoon model, while the black
 314 line indicates the measured data at the gauge stations. (a) and (b) Winnie. (c) and (d) Wipha at Daji and Tanxu Stations
 315





316 **Fig. 6** Data comparison between computed wind direction (degree) and observed data at the two wind gauge stations in
 317 Shanghai during Typhoon Winnie and Wipha. The blue line presents the simulated results from the typhoon model, while the
 318 black line indicates the measured data at the gauge stations. (a) and (b) Winnie. (c) and (d) Wipha at Daji and Tanxu
 319 Stations.

320

321 4.3 Results of the Shanghai Coastal Typhoon Storm Surge Model (SC-TSSM)

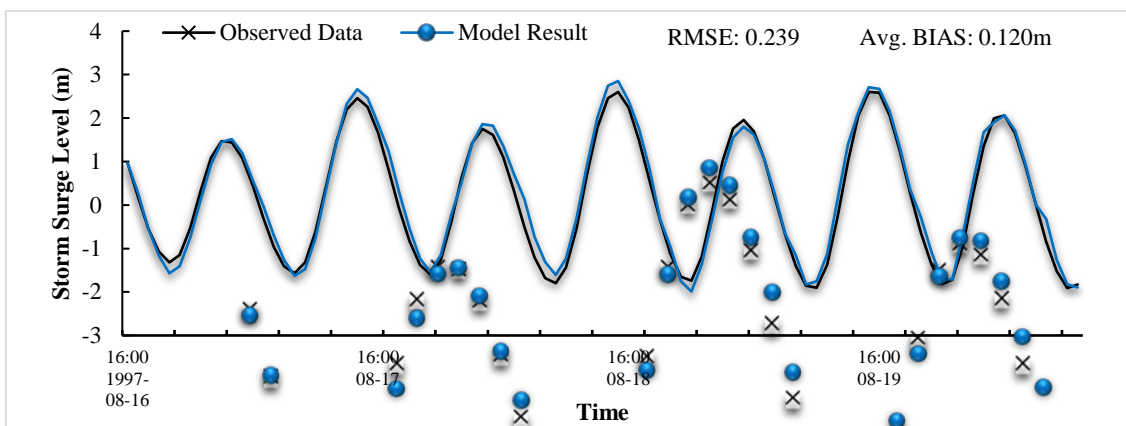
322 The typhoon simulation results were used as input into a storm surge model to provide the wind profile. In order to simulate a
 323 typhoon-generated storm surge at coastal and regional scales, a Shanghai Coastal Typhoon Storm Surge Model (SC-TSSM)
 324 was developed here. In this section, the configuration, validation, and calibration of the SC-TSSM will be described in detail,
 325 and the simulated results of a storm surge caused by two selected typhoon will be discussed accordingly. SC-TSSM covers the
 326 Shanghai coastal area between latitudes 27 -35° N and longitudes 120 – 128° E with varying domain resolutions from 1 – 100
 327 km (Fig. 3).

328 This unstructured-grid high-resolution model has been developed to satisfy the computation requirements during storm surge
 329 simulation, within the geographic coverage of the Shanghai sea and coastal area. This model system contains both the Shanghai
 330 Coastal Typhoon Storm Surge Model (SC-TSSM) and the regional Hengsha Island Typhoon Storm Surge Model (HI-TSSM).
 331 Multiple physical factors are included in this model system, such as typhoon events, open ocean currents, astronomical tides,
 332 surface waves and freshwater discharge. Surface Water Modelling System (SMS) was used to generate mesh for this study
 333 since it has a more effective grid generation function than MIKE, and it can refine a flexible mesh gradually which cannot be
 334 achieved in MIKE.

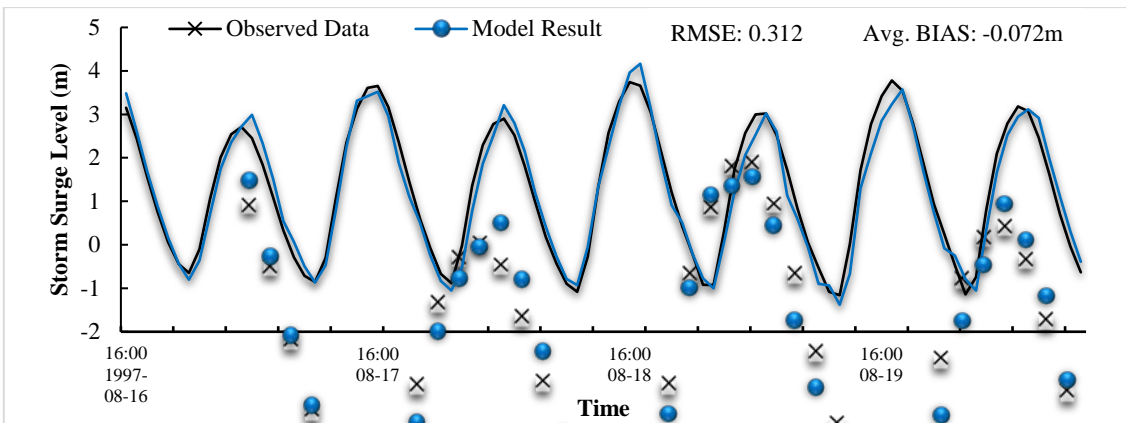
335 In this model, the effect of different shapes of the sea wall in the storm surge model is small, therefore the shape of the sea wall
336 wall was assumed to be trapezoidal. The height of the sea wall along the Shanghai coastline has been set to 6.37 m relative to
337 mean sea level. The manning number was chosen as the bed resistance factor, and it was set to $80 \text{ m}^{1/3}/\text{s}$ for ocean and $32 \text{ m}^{1/3}/\text{s}$
338 for land area. For wind forcing, the input wind profile was generated from the computed results of typhoon model, including
339 air pressure and U/V component of wind velocity that varied in time and domain. Since the Yangtze Estuary is included in the
340 SC-TSSM, the river's discharge should be taken into consideration as a source of freshwater. Based on previous work, the
341 discharge of Yangtze River has been set to $45\,000 \text{ m}^3/\text{s}$ as the mean discharge for the period of July-September (Ge 2010).

342 As shown in Fig. 7, the results suggest that the SC-TSSM can simulate the propagation of storm surge satisfactorily. In general,
343 the numerical computation results are in good agreement with the observations, although some sections of the simulation are
344 under-predicted. For example, the differences between computation and observation are in the range of 0.2 – 0.5 m from 17 to
345 19 September 2007.

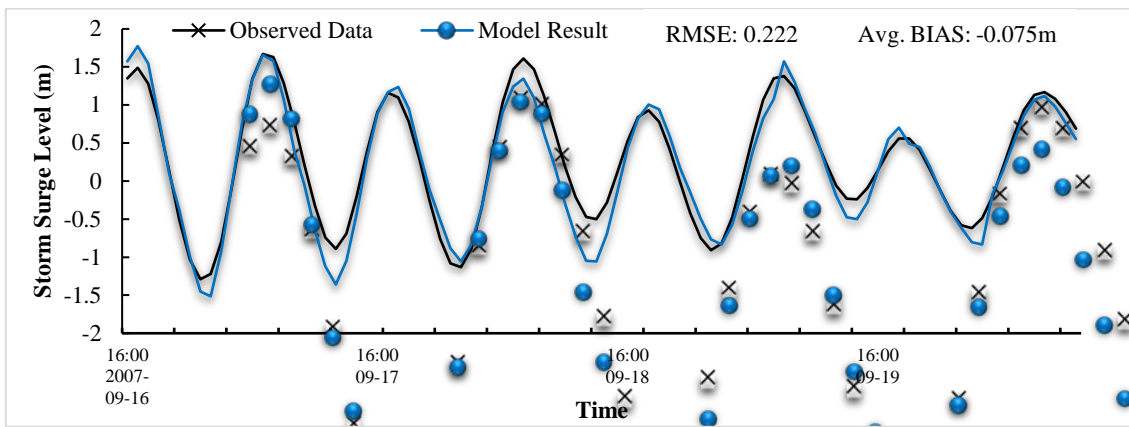
346



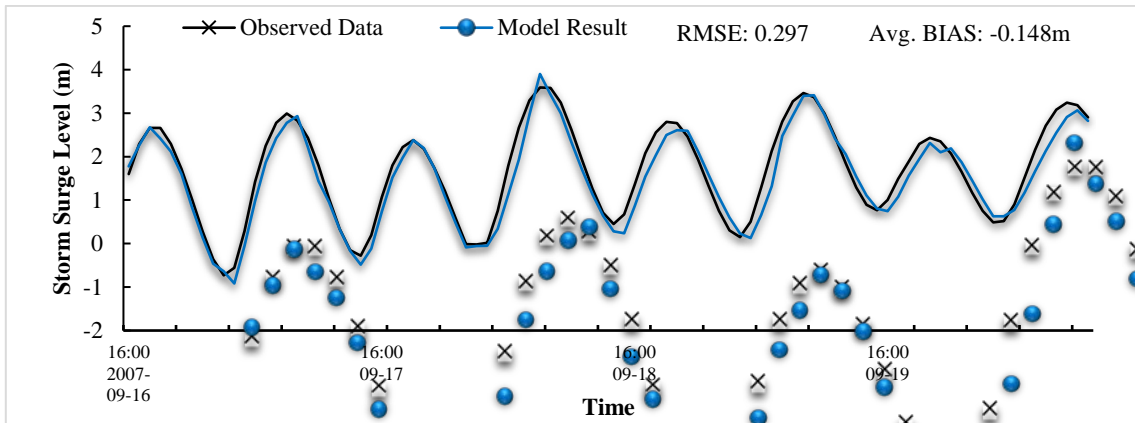
(a) Typhoon Winnie at Daji Station



(b) Typhoon Winnie at Tanxu Station



(c) Typhoon Wipha at Daji Station

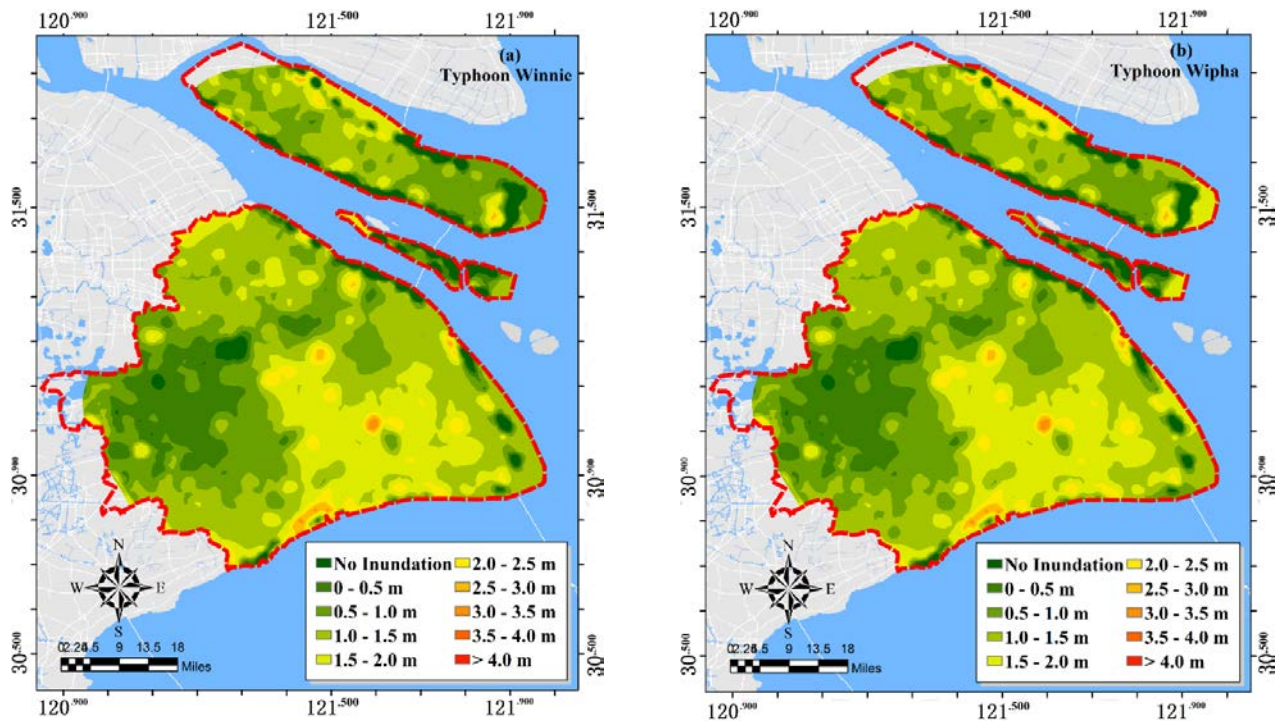


(d) Typhoon Wipha at Tanxu Station

347 **Fig. 7** Comparison of the observation data (black) and simulated results (blue) of storm surge levels (a) and (b) during
 348 Typhoon Winnie and (c) and (d) during Wipha at Daji and Tanxu stations.

349

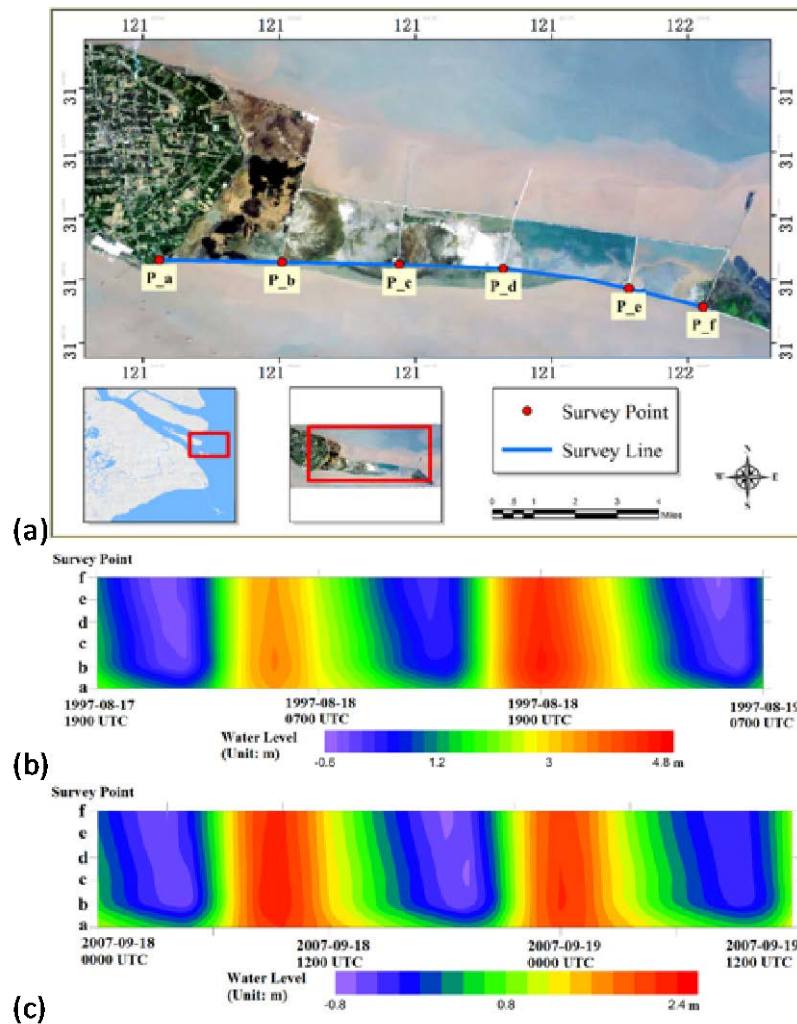
350 Based on simulation results from MIKE 21, distribution maps of storm surge inundation and inundation depth in Shanghai,
 351 during the two case study typhoon events, are presented in Fig. 8. Simulation results show both typhoon gave rise to storm
 352 surge inundation in Shanghai across a large area. The distribution of storm surge inundation caused individually by Winnie
 353 and Wipha was basically the same but with a few differences in flood depth observed along the coastline and on the east and
 354 north coasts of Chongming and Hengsha Islands. The average inundation levels from the storm surge that occurred during
 355 these two typhoon, were 1.78 m in 1997 (Winnie) and 0.9 m in 2007 (Wipha) in eastern Shanghai.



356 **Fig. 8** Distribution of the Maximum Inundation Area and Depth over Shanghai During (a) Typhoon Winnie and (b) Wipha

357

358 In order to analyse the effect of storm surge may have on reclamation projects around Hengsha Island, a survey line and six
 359 survey points along the south bank of the on-going project have been drawn (Fig. 9(a)). As the tide moved toward the south
 360 bank of Hengsha Island the time series of water level at these survey points can reveal the variation characteristics of storm
 361 surge in this area. The water level and wave speed at these six survey points have been extracted from simulations in the HI-
 362 TSSM (Hengsha Island Tropical Storm Surge Model). An hourly output from the HI-TSSM for the period from 18 hours
 363 before the landfall of the typhoon to 12 hours after demonstrates the differences of surge elevation and speed between the
 364 different locations (Fig. 9(b) and (c)).



365

366 **Fig. 9** (a) Location of the survey line (blue) and six survey points (red) along the south bank of the reclamation project around
 367 Hengsha Island, and distribution of water level (m) at the survey points during (b) Winnie and (c) Wipha. Sources: Esri,
 368 DigitalGlobe, GeoEye, i-cubed, USDA FSA, USGS, AEX, Getmapping, Aerogrid, IGN, IGP, swisstopo, and the GIS User
 369 Community

370

371 Water levels at these survey points decreased slightly from points a to f. Differences in water level between these selected
 372 points were larger during low tide than high tide. The difference between points a and f was 0.72 m (Winnie) and 0.52 m
 373 (Wipha) at high tide, while it was up to 1.79 m and 1.32 m respectively during low tide (Fig. 8(c)). Coastal vulnerability to
 374 typhoon storm surge inundation defined in this study is sensitive to the elevation of storm surge, especially during high tide.
 375 Therefore, although there are only slightly differences in surge level (0.52 – 1.79 m between points a and f) along the survey
 376 line, will lead to a variation of coastal inundation vulnerability to storm surge. The results also imply that vulnerability of land
 377 reclamation to typhoon storm surge varies from place to place. Therefore it is important to analyse coastal vulnerability to
 378 storm surge inundation of reclaimed land before allocating different land use types. Better understanding of such vulnerability
 379 will also provide crucial support to stakeholders for them to generate sustainable effective coastal protection strategies.

380 Generally, the mouth of Yangtze River, Hangzhou Bay, Chongming, and Hengsha Islands, and the river bank along the Dazhi
 381 and Huangpu Rivers were the most seriously affected areas during these typhoon storm surge inundations. The inundation
 382 depths at these places were usually over 1.0 m. Maximum inundation depth in those areas reached 3.82 m during Winnie, and

383 2.65 m during Wipha. Severe storm surge led to widespread flooding, and the airport, factories, and warehouse, commercial
384 and residential buildings were flooded. Combined with heavy rainfall, this meant the transportation system was disrupted,
385 including communication lines and international airports. The detailed information on storm surge inundation in Shanghai
386 during Winnie and Wipha were not available, thus the oceanic disaster communique of China published by State Oceanic
387 Administration (1989-2015) was utilized to validate the inundation situation in Shanghai. The simulation results were in good
388 agreement with the published descriptions, and in line with previous studies in Shanghai (Chen and Wang 2000; French 2001;
389 Hu et al. 2005; Hu and Jin 2007; Ge 2010; Yin 2011; Yin et al.,2013a; Harwood et al. 2014).

390 The results from this study also suggested that the height of storm surge along the Huangpu River and Dazhi River basin was
391 high and the river banks experienced serious flooding during typhoon induced storm surge, which was also reported by the
392 oceanic disaster communique of China published by State Oceanic Administration (1989-2015). Previous studies failed to
393 capture these features (Chen and Wang 2000; French 2001; Hu et al. 2005; Hu and Jin 2007; Ge 2010; Yin 2011; Yin et al.
394 2013a; Harwood et al. 2014).

395

396 **5 Discussion**

397 For typhoon storm surge modelling in this study we demonstrate that a meso-scale simulation can be used to compute storm
398 surge inundation and assess the inundation vulnerability of different land use types. This study enlarges the body of knowledge
399 on storm surge studies in Shanghai, and also proposes a meso-scale simulation can be used for coastal planning purposes.
400 Previous studies of storm surge were usually conducted at national or local levels (Dietrich et al. 2011b; Butler et al. 2012;).
401 In China, most of these studies tended to emphasize the significance of numerical modelling of storm surge and risk analysis
402 either for the coastline on a large spatial scale (>100 km in length) (Zheng 2010; Tan et al. 2011; Yin 2011;) or for the small
403 scale coastal area (1 – 1000m in length) with fine resolution simulation (Zhang et al. 2006; Xie 2010; Xie et al. 2010; Ye 2011.
404 The majority of these studies concentrated on three districts in the Shanghai coastal area, namely, the Pudong, Jinshan, and
405 Fengxian Districts (Xie 2010; Ye 2011). These studies probably needed to pay more attention to the river basins. However,
406 results from this study show that the river basins of the Dazhi and Huangpu Rivers were among the most serious impacted
407 areas during Typhoon Winnie and Wipha. Meso-scale (1 – 100 km in length) studies on storm surge have not been conducted
408 for Shanghai, and the meso-scale framework in this study fills the gap.

409 Large and small-scale simulations do each have their own advantages. For example, large-scale simulations require low
410 consumption of computation resources and time depending on the resolution used. Large-scale studies therefore could be
411 applied on a national scale to analyse typhoon storm surge impacts, to simulate typhoon and storm surge changes over time,
412 and to provide necessary data to propose general plans for hazard mitigation. Small-scale simulations usually involve fine
413 spatial resolutions, ranging from 5 m to 100 m, in order to capture subtle changes of the flood waters. Nonetheless, neither
414 large nor small-scale simulations always fit for coastal planning purposes. Large-scale simulation is not suitable for local
415 planning because its coarse spatial resolution cannot reflect the detailed distribution of storm surge inundation. Although
416 numerical simulation, in the context of coastal planning, requires a significant number of accurate and detailed computation
417 results at a regional level, high spatial resolution at the local scale will have high costs in terms of computation resource and
418 time. For example, a small-scale model with a fine spatial resolution mesh of 100 m – 1 km was initially used in this study,
419 covering only the estuary and coastal area. It required over 600 hours to run one simulation on a computer with 16G RAM,
420 500G SSD, quad-core Intel Core i5 processors. Compared to the 600 hours of computation time by small scale model, the
421 multi-nested meso-scale model only required about 30 hours to run a single simulation with a reasonable accuracy where
422 required. Meso-scale studies could therefore not only fulfil the requirements for simulation accuracy, but also take less time

423 and resource. They are more suitable for use when a large number of simulations are required over a long-time scale. By
424 implementing this meso-scale model, the focus of storm surge simulation is at an appropriate medium scale to fit planning
425 purposes.

426 The simulations conducted in this study has enlarged the body of knowledge about storm surge inundation in Shanghai, and
427 suggested that more attention needs to be paid not only to the area along the coastline, but also to the nearby rivers. Some
428 studies in Shanghai started to look at the inundation along Huangpu River caused by typhoon storm surge (Borsje et al. 2011;
429 Yin et al. 2013a). Globally, the work conducted by Rupp and Nicholls (2002) on the river Thames emphasized the interaction
430 of surge and tide in river basin. Ali (1996) also demonstrated in their study that the most severe inundation area during a
431 synthetic typhoon in eastern North Carolina was in the Pamlico River region.

432 **6 Conclusions**

433 This paper developed a resource and time efficient approach for simulating typhoon-generated storm surge, which can be
434 applied to coastal mega-cities around the world, even where flood observation data is inadequate. Typhoon induced storm
435 surge was simulated in Shanghai and inundation maps were drawn in ArcGIS. These maps provide a clearer picture of the
436 spatial distribution and the variation of such vulnerability over Shanghai. Results showed the south of Shanghai, the river
437 banks along the Huangpu and Dazhi Rivers and most of Chongming Island were subject to serious typhoon storm surge
438 inundation. It also showed that reclamation land, such as that on Hengsha Island is particularly vulnerable to storm surge
439 innundation. The meso-scale simulation method proposed in this study provides a realistic storm-surge innundation result at
440 the city level. Furthermore, due to its low data and time consumption, this approach can be implemented when a large number
441 of models are required for mitigation and planning.

442 **Author Contribution**

443 Dong, Stephenson and Wakes devised the numerical experiments. Dong carried out the numerical simulations and analysis of
444 the results. Chen and Ge supplied the validation data, commented and advised on model construction and outputs. Dong,
445 Stephenson and Wakes prepared the manuscript.

446 **Acknowledgements**

447 The authors would like to acknowledge the University of Otago PhD scholarship that funded this work and DHI for access to
448 MIKE 21.

449 **References**

- 450 Aerts JC, Botzen WW, Emanuel K, Lin N, de Moel H, Michel-Kerjan EO (2014) Evaluating flood resilience strategies for
451 coastal megacities *Science* 344:473-475
- 452 Bode L, Hardy TA (1997) Progress and recent developments in storm surge modeling *Journal of Hydraulic Engineering*
453 123:315-331
- 454 Butler T, Altaf M, Dawson C, Hoteit I, Luo X, Mayo T (2012) Data assimilation within the advanced circulation (ADCIRC)
455 modeling framework for hurricane storm surge forecasting *Monthly Weather Review* 140:2215-2231
- 456 Chen Q, Wang S (2000) Storm-tide disaster and its forecast in Shanghai city *Journal of Catastrophology* 15:26-29
- 457 Choi BH, Eum HM, Woo SB (2003) A synchronously coupled tide-wave-surge model of the Yellow Sea Coastal Engineering
458 47:381-398 doi:[http://dx.doi.org/10.1016/S0378-3839\(02\)00143-6](http://dx.doi.org/10.1016/S0378-3839(02)00143-6)
- 459 Davis JR, Paramygin VA, Forrest D, Sheng YP (2010) Toward the probabilistic simulation of storm surge and inundation in
460 a limited-resource environment *Monthly Weather Review* 138:2953-2974
- 461 Dietrich JC et al. (2012) Performance of the unstructured-mesh, SWAN+ ADCIRC model in computing hurricane waves and

462 surge *Journal of Scientific Computing* 52:468-497

463 Dietrich JC et al. (2011a) Modeling hurricane waves and storm surge using integrally-coupled, scalable computations *Coastal*

464 *Engineering* 58:45-65

465 Dietrich JC et al. (2011b) Hurricane Gustav (2008) waves and storm surge: hindcast, synoptic analysis, and validation in

466 *Southern Louisiana Monthly Weather Review* 139:2488-2522

467 Dutta D, Herath S, Musiak K (2003) A mathematical model for flood loss estimation *Journal of hydrology* 277:24-49

468 Elsaesser B, Bell A, Shannon N, Robinson C (eds) (2010) Storm surge hind-and forecasting using Mike21FM-Simulation of

469 surges around the Irish Coast. Proceedings of the International MIKE by DHI Conference—Modelling in a World of

470 Change, Copenhagen, Denmark. , Copenhagen, Denmark

471 Flather R, Smith J, Richards J, Bell C, Blackman D (1998) Direct estimates of extreme storm surge elevations from a 40-year

472 numerical model simulation and from observations *The Global Atmosphere and Ocean System* 6:165-176

473 Frazier TG, Wood N, Yarnal B, Bauer DH (2010) Influence of potential sea level rise on societal vulnerability to hurricane

474 storm-surge hazards, Sarasota County, Florida *Applied Geography* 30:490-505

475 French PW (2001) Coastal defences: processes, problems and solutions Psychology Press

476 Funakoshi Y, Hagen SC, Bacopoulos P (2008) Coupling of hydrodynamic and wave models: Case study for Hurricane Floyd

477 (1999) hindcast *Journal of waterway, port, coastal, and ocean engineering* 134:321-335

478 Ge J (2010) Multi Scale FVCOM Model System for the East China Sea and Changjiang Estuary and Its Applications. Shanghai:

479 East China Normal University

480 Ge J, Ding P, Chen C, Hu S, Fu G, Wu L (2013) An integrated East China Sea–Changjiang Estuary model system with aim at

481 resolving multi-scale regional–shelf–estuarine dynamics *Ocean Dynamics* 63:881-900

482 Harper B, Holland G An updated parametric model of the tropical cyclone. In: Proc. 23rd Conf. Hurricanes and Tropical

483 Meteorology, 1999.

484 Harwood S, Carson D, Wensing E, Jackson L (2014) Natural hazard resilient communities and land use planning: the

485 limitations of planning governance in tropical Australia *Journal of Geography & Natural Disasters* 4:1-15

486 Holland GJ (1980) An analytic model of the wind and pressure profiles in hurricanes *Monthly weather review* 108:1212-1218

487 Huang Y, Weisberg RH, Zheng L (2010) Coupling of surge and waves for an Ivan-like hurricane impacting the Tampa Bay,

488 Florida region. *Journal of Geophysical Research* 115: C12009.

489

490 Hu C, Jin Y (2007) Storm surge disaster in Shanghai: Quasi-periodicity and prediction *Urban Roads Bridges & Flood Control*

491 26-29

492 Hu D, Gong, M, Yazhen, K (2005) Study of the influence of strong storm surges in Shanghai *Journal of East China Normal*

493 *University (Natural Science)* 177-182

494 Jakobsen F, Madsen H (2004) Comparison and further development of parametric tropical cyclone models for storm surge

495 modelling *Journal of Wind Engineering and Industrial Aerodynamics* 92:375-391

496 Jia A, Wang Y, Yang Q (2011) Research on Inundation Loss Assessment Model for Farmland *Journal of Water Resources and*

497 *Architectural Engineering* 6:006

498 Jiang Y, Kirkman H, Hua A (2001) Megacity development: managing impacts on marine environments *Ocean & Coastal*

499 *Management* 44:293-318

500 Lowe J, Gregory J, Flather R (2001) Changes in the occurrence of storm surges around the United Kingdom under a future

501 climate scenario using a dynamic storm surge model driven by the Hadley Centre climate models *Climate dynamics*

502 18:179-188

503 Molteni F, Buizza R, Palmer TN, Petroliagis T (1996) The ECMWF ensemble prediction system: Methodology and validation

504 *Quarterly journal of the royal meteorological society* 122:73-119

505 Ogie R.I., Adam C., Perez P.: A review of structural approach to flood management in coastal megacities of developing nations:

506 current research and future directions *Journal of Environmental Planning and Management*, 63:127-147, 2019.

507 Rankine WJM (1872) A manual of applied mechanics. Charles Griffin and Company,

508 Savioli J, Pedersen C, Szykarski S, Kerper D Modelling the threat of tropical cyclone storm tide to the Burdekin Shire,

509 Queensland Australia. In: Coasts & Ports 2003 Australasian Conference: Proceedings of the 16th Australasian Coastal

510 and Ocean Engineering Conference, the 9th Australasian Port and Harbour Conference and the Annual New Zealand

511 Coastal Society Conference, 2003. Institution of Engineers, Australia, p 285

512 Shanghai Municipal Planning and Land & Resources Administration (2010) Shanghai Master Plan (2010-2030). Shanghai

513 Municipal Planning and Land & Resources Administration, Shanghai

514 Shanghai Nongken Chronicles Compilation Committee (2004) Shanghai Nongken Chronicles. Shanghai Academy of Social

515 Sciences Press, Shanghai

516 Sheng YP, Zhang Y, Paramygin VA (2010) Simulation of storm surge, wave, and coastal inundation in the Northeastern Gulf

517 of Mexico region during Hurricane Ivan in 2004 *Ocean Modelling* 35:314-331

518 Shepard CC, Agostini VN, Gilmer B, Allen T, Stone J, Brooks W, Beck MW (2012) Assessing future risk: quantifying the

519 effects of sea level rise on storm surge risk for the southern shores of Long Island, New York *Natural Hazards* 60:727-

520 745

521 Simmons A, Uppala S, Dee D, Kobayashi S (2007) ERA-Interim: New ECMWF reanalysis products from 1989 onwards

522 *ECMWF newsletter* 110:25-35

523 Smagorinsky J (1963) General circulation experiments with the primitive equations: I. the basic experiment* *Monthly weather*

524 *review* 91:99-164

525 State Oceanic Administration PsRoC (1989-2015) The oceanic disaster communique of China.

526 Tan L, Chen K, Wang J, Yu L (2011) Assessment on storm surge vulnerability of coastal regions during the past twenty years
527 *Scientia Geographica Sinica* 31:1111-1117

528 Timmerman P, White R (1997) Megahydropolis: coastal cities in the context of global environmental change *Global*
529 *Environmental Change* 7:205-234

530 Vickery PJ, Skerlj P, Steckley A, Twisdale L (2000) Hurricane wind field model for use in hurricane simulations *Journal of*
531 *Structural Engineering* 126:1203-1221

532 Wamsley TV, Cialone MA, Smith JM, Ebersole BA, Grzegorzewski AS (2009) Influence of landscape restoration and
533 degradation on storm surge and waves in southern Louisiana *Natural Hazards* 51:207-224

534 Westerink JJ et al. (2008) A basin-to channel-scale unstructured grid hurricane storm surge model applied to southern
535 Louisiana *Monthly Weather Review* 136:833-864

536 Woodruff JD, Irish JL, Camargo SJ (2013) Coastal flooding by tropical cyclones and sea-level rise *Nature* 504:44-52

537 Xie C (2010) Risk assessment and scenario simulation of storm surge in Shanghai coastal areas. East China Normal University

538 Xie C, Hu B, Wang J, Chen J, Xu S, Liu Y, Ye M (2010) Risk assessment and floodplain scenarios of storm surge of Tianjin
539 Binhai area *Transactions of Oceanology and Limnology* 2:130-140

540 Xie L, Liu H, Peng M (2008) The effect of wave-current interactions on the storm surge and inundation in Charleston Harbor
541 during Hurricane Hugo 1989 *Ocean Modelling* 20:252-269

542 Ye M (2011) Compounded scenarios simulation and emergency evacuation of storm surge disaster in coastal cities. East China
543 Normal University

544 Yeung Y-m (2001) Coastal mega-cities in Asia: transformation, sustainability and management *Ocean & Coastal Management*
545 44:319-333

546 Yin J (2011) Study on the risk assessment of typhoon storm tide in China coastal area. East China Normal University

547 Yin J, Yu D, Yin, Z, Wang, J, Xu, S (2013) Modelling the combined impacts of sea-level rise and land subsidence on storm
548 tides induced flooding of the Huangpu River in Shanghai, China *119:919-932*

549 Ying M et al. (2014) An overview of the China Meteorological Administration tropical cyclone database *Journal of*
550 *Atmospheric and Oceanic Technology* 31:287-301

551 Young I, Sobey R (1981) The numerical prediction of tropical cyclone wind-waves. Department of Civil & Systems
552 Engineering, James Cook University of North Queensland,

553 Zhang K, Xiao C, Shen J (2008) Comparison of the CEST and SLOSH models for storm surge flooding *Journal of Coastal*
554 *Research*:489-499

555 Zhang X, Zhang W, Liu Y, Qiu S (2006) Simulation models of flood inundation due to storm tide *Journal of System Simulation*
556 18:20-23

557 Zheng L (2010) Development and application of a numerical model coupling storm surge, tide and wind wave. Doctor of
558 Engineering, Tsinghua University

559 Zheng L et al. (2013) Implications from the comparisons between two - and three - dimensional model simulations of the
560 Hurricane Ike storm surge *Journal of Geophysical Research: Oceans* 118:3350-3369

561 Zhu P, Chen M, Tao Z, Wang H (2002) Numerical simulation of Typhoon Winnie (1997) after landfall. Part I: Model
562 verification and model clouds *Acta Meteor Sinica* 60:553-559

563

564

565

566

567

568

569

570

571 **Table 1** Major configuring parameters for the simulation models

Model Parameter	Configuration
Minimum Time Step	0.01 sec
Maximum Time	30 secs
Critical CFL Number	0.8
Drying Depth	0.005 m
Flooding Depth	0.05 m
Wetting Depth	0.1 m
Manning Number	80 m ^{1/3} /s for ocean, 32 m ^{1/3} /s for land
Neutral Pressure of Wind Field	1008 hPa
Soft Start Interval for Wind	3600 secs
Freshwater Discharge	Simple Source, 45 000 m ³ /s

572